Scientiae Radices, **3**(3), 157-186 (2024)

Full Paper

Dedication to Prof. Robert G. Parr for his contribution to the study of chemical organic reactivity.

SciRad SCIENTIAE RADICES

1999 – 2024, a Quarter Century of the Parr's Electrophilicity ω Index

Luis R. Domingo ✉

Department of Organic Chemistry, University of Valencia, Dr. Moliner 50, 46100 Burjassot, Valencia, Spain

✉ Correspondence to: luisrdomingo@gmail.com

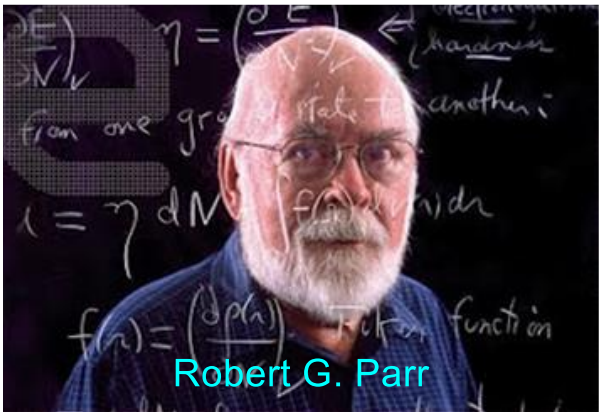

Abstract: In 1999, Robert G. Parr introduced the electrophilicity ω index as a measure of the electronic stabilization of a molecule when it acquires an additional amount of electron density. Numerous theoretical studies over the last 25 years have demonstrated the usefulness of this index in the study of polar reactions. The present MEDT study reinforces the relevance of Parr's electrophilicity ω index as a quantitative measure of the electrophilic character of species involved in polar reactions.

Keywords: Electrophilicity ω index, reactivity indices, polar reactions, MEDT

Received: 2024.07.16
Accepted: 2024.08.30
Published: 2024-09-03
DOI: 10.58332/scirad2024v3i3a02

Introduction

Organic reactions are classified as non-polar and polar reactions. While non-polar reactions are experienced mainly by saturated hydrocarbons, unsaturated hydrocarbon compounds and organic molecules contain C–X, C=X, and C≡X functional groups, where X is a heteroatom, experience polar reactions. Non-polar reactions usually present high activation energies, while polar reactions present low activation energies, which depend on the polar character of the reaction; i.e., when more polar, faster the reaction.

The concept of polar reactions in Organic Chemistry was developed at the beginning of the past century. Unlike Inorganic Chemistry, which is associated mainly with ionic species, Organic Chemistry is associated with molecular compounds. This important structural difference also causes a different reactivity; while the chemistry of the ionic species is mainly thermodynamically controlled, that of molecular compounds is kinetically controlled as it demands changes in the ground state electronic structure associated with the rupture and formation of new bonds.

The polar character of the reactions depends on the electrophilicity and the nucleophilicity of the reagents. The electrophile and nucleophile concepts were introduced by K. Ingold [1], who replaced the terms 'anionoid' and 'cationoid' proposed earlier by A. J. Lapworth in 1925 [2]. Ingold proposed the nucleophilic (nucleus-seeking) and electrophilic (electron-seeking) species as a generalization of the concepts of bases and acids, defined by Lewis as species, the neutralization of which involves the donation or acceptance of an electron-pair. However, while nucleophilicity and electrophilicity emphasize the kinetic aspect of reactivity, Lewis's basicity and acidity emphasize the thermodynamic aspect of the Lewis adduct formation.

From an experimental point of view, in 1993 Mayr and Patz proposed electrophilicity/ nucleophilicity scales [3] based on the rate constants for a large list of electrophile /nucleophile combination reactions. Mayr and co-workers found that the kinetic rate constants of electrophiles and nucleophiles obey the relationship $\log k = s\,(E + N)$, where electrophiles are characterized by the E parameter, and nucleophiles are characterized by two parameters, N and s, the last being the nucleophile specific slope parameter [3]. On this basis, these authors developed experimental electrophilicity and nucleophilicity scales for a great diversity of organic and organometallic compounds [4,5,6].

In the period 1995-2000, Domingo began the theoretical study of organic reactions, more specifically in Diels-Alder (DA) and [3+2] cycloaddition (32CA) reactions. A relationship between the expected nucleophilic character of the diene or the three-atom-components (TACs), and the expected electrophilic character of the ethylene, or vive-versa, and the

computed activation energies could be established. In this period, the charge transfer calculated at the transition state structure (TSs) was used as a physical property characterizing these stationary points.

In 1999, the DA reactions between nitroethylene **1** and three substituted ethylenes of increased nucleophilic character (propene **2**, methyl vinyl ether **3**, and dimethylvinylamine **4**), in the absence and presence of Lewis acid catalysts were theoretically studied (see Scheme 1) [7]. The activation energies of these DA reactions decreased with the increase of the expected nucleophilic character of the ethylene, **2** < **3** < **4**. A good correlation was established between the decrease of the activation energies and the increase of the global electron density transfer [8] (GEDT) at the TSs.

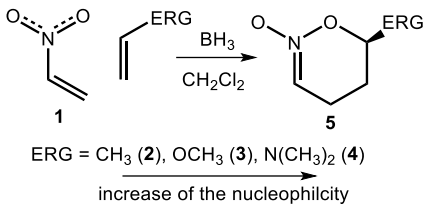

Scheme 1. DA reactions between nitroethylene **1** and propene **2**, methyl vinyl ether **3**, and dimethylvinylamine **4**, in the absence and presence of BH_3 catalyst.

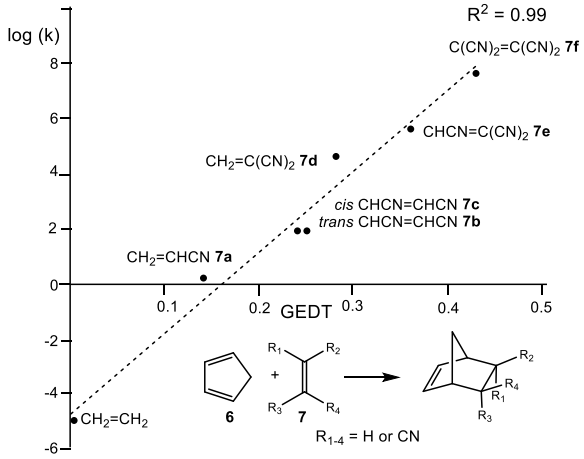

Fig. 1. Plot of the logarithm of the experimental rate constant k vs. GEDT, in average number of electrons, e, for the DA reactions of Cp **1** with the cyanoethylene series **7**.

Further, in 2002, a linear correlation between the GEDT taking place at the TSs involved in the DA reactions of cyclopentadiene **6** with the cyano ethylene series **7**, and the experimental relative reaction rates reported by Sustman in 1964 [9] was established (see Figure 1) [10]. Note that the concept of GEDT was introduced in 2014 by Domingo against the concept of charge transfer [8]. These findings allowed in 2009 to establish the mechanism of the polar Diels-Alder reactions, which are controlled by the

nucleophilic/electrophilic interactions taking place at the TSs, and not for frontier molecular orbital (MO) interactions [11].

In the late 1970s and early 1980s Robert G. Parr developed the so-called Conceptual Density Functional Theory (CDFT) [12]. CDFT tries to extract from the electron density relevant concepts and principles that make it possible to understand and predict the chemical behavior of a molecule. Two significant CDFT indices proposed by Parr are the electronic chemical potential μ [13], which provides tendency of an electrophile to acquire an extra amount of electron density, and the chemical hardness η [14] which provides a measure of the resistance of a molecule to exchange electron density.

Latter, in 1999, Parr proposed the electrophilicity ω index [15], which gives a measure of the energy stabilization of a molecule when it acquires an additional amount of electron density, ΔN, from the environment. The electrophilicity ω index is given by the simple expression:

$$\omega = \frac{\mu^2}{2\eta} \tag{1}$$

Thus, a good electrophile is a species characterized by a high $|\mu|$ value and a low η value. Considering that the electronegativity χ is the negative of the electronic chemical potential μ, $\chi = -\mu$, and that the softness S is the inverse of the hardness η, $S = 1/\eta$, a good electrophilic molecule is characterized to be a high electronegative and soft species.

In the CDFT, the electronic chemical potential μ and the chemical hardness η were approximated as $\mu \approx -(I + A) / 2$ and $\eta \approx (I - A) / 2$, where I is the ionization potential and A the electron affinity. By using the Koopmans' theorem [16] and the Kohn–Sham (KS) formalism [17], these energies can be approached within the Hohenberg and Kohn Density Functional Theory (DFT) [18] by the frontier KS HOMO and LUMO energies where I by $-E_{HOMO}$ and A by $-E_{LUMO}$.

The Parr's electrophilicity ω index has become a powerful tool for the study of the reactivity of organic molecules participating in polar reactions [19,20]. A comprehensive study carried out in 2002 on the electrophilicity of a series of molecules participating in DA reactions allowed establishing a single electrophilicity ω scale (see Table 1) [21]. This scale allowed the classification of organic molecules as strong electrophiles with $\omega \geq 1.50$ eV, moderate electrophiles with $0.80 \leq \omega < 1.50$ eV and marginal electrophiles with $\omega < 0.80$ eV [21]. Further, species with $\omega \geq 4.00$ eV were classified as superelectrophiles [20].

Table 1. B3LYP/6-31G(d) electrophilicity ω index, in eV, of some common reagents involved in Diels-Alder reactions.

Molecules	ω
Strong electrophiles	
$CH_2=N^+(CH_3)_2$	8.25
$(CN)_2C=C(CN)_2$	5.96
$CH_2=CHCHO:BH_3$	3.20
$CH_2=C(CN)_2$	2.82
$CH_2=CHNO_2$	2.61
$CH_2=CHCHO$	1.84
$CH_2=CHCN$	1.74
$CH_2=CHCOCH_3$	1.65
$CH_2=CHCO_2CH_3$	1.51
Moderate electrophiles	
$CH_2=CH-CH=CH_2$	1.05
$CH_2=CH(CH_3)-CH=CH_2$	0.94
Cyclopentadiene	0.83
Marginal electrophiles (Nucleophiles)	
$CH_3O-CH=CH-CH=CH_2$	0.77
$CH_2=CH_2$	0.73
$(CH_3)_2N-CH=CH-CH=CH_2$	0.57
$CH\equiv CH$	0.54
$CH_2=CHOCH_3$	0.42
$CH_2=CHN(CH_3)_2$	0.27

It is important to consider some pertinent questions to understand the applicability of the Parr's electrophilicity ω index in the study of polar organic reactions: i) the polar character of an organic reactions is mainly determined by the electrophilic character of a reactive (see later). For practical purposes, an electrophile should have an electrophilicity ω ≥ 2.00 eV. Molecules with ω < 1.50 eV, classified as moderate electrophiles, practically do not participate as electrophiles in polar processes; ii) the ω index is a measure of the maximum stability of a species when it receives the maximum electron density of the environments. Consequently, the stabilization of an electrophile at the TS of a polar reaction is dependent on the amount of electron density provided by the nucleophile; and iii) the electrophilicity ω index is a global property of a molecule, while the reactivity, i.e. formation of new bonds, is a local property. Thus, there are strong electrophilic species such as *p*-nitrophenyl azide **8**, ω = 2.66 eV, which acts as a poor electrophile in polar 32CA reactions toward nucleophilic species [22]. This behavior is a consequence of the fact that the electrophilicity of this phenyl azide is mainly concentrated on the *p*-nitrophenyl substituent, while the –NNN azide framework is poorly electrophilically activated [22]. In this sense, the analysis of the electrophilic Parr P_k^+ functions [23] give a measure of the electrophilic centers

of a molecule. Figure 2 shows the analysis of the electrophilic Parr P_k^+ functions at the *p*-nitrophenyl azide **8**; as can be seen, the electrophilic Parr P_k^+ function of the terminal nitrogen atom of the azide framework is only 0.15.

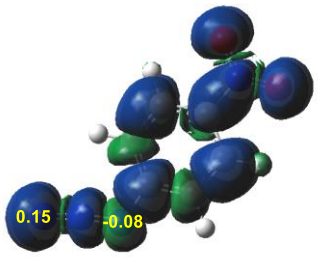

8

Fig. 2. 3D representations of the Mulliken atomic spin densities of the radical anion of azide **8**, including the corresponding electrophilic P_k^+ Parr functions.

Due to the relevance of the nucleophilic character of a molecule to favor the electron density donation to an electrophile in a polar reaction, in 2008 Domingo et al. proposed an empirical nucleophilicity *N* index based on the ionization potential I of a molecule. Taking in account the Koopmans theorem [16], the nucleophilicity *N* index is given by the simple expression [24]:

$$N = E_{HOMO(Nu)} - E_{HOMO(TCE)} \quad (2)$$

where $E_{HOMO(Nu)}$ is taken as an approximation to I of the nucleophile. As tetracyanoethylene **9** (TCE) is a species with a very negative I value, this energy reference is used to hand the nucleophilicity scale of positive values [24]. Many studies of organic reactions carried out in the last years proved that the analysis of the electrophilicity ω index and nucleophilicity *N* indices at the ground state of the reagents is a powerful tool to predict the polar character of a reactions, and consequently, its feasibility [20,25]. Thus, an experimental polar reaction requires the participation of a strong electrophile with a $\omega \geq 2.00$ eV and a strong nucleophile with a $N \geq 3.00$ eV to take place. Herein, it is important to note that in CDFT the values of the KS HOMO and LUMO energies are chosen as an approximation to the I and A energies of a molecule, but any analysis of the symmetry of the corresponding KS MOs is done as in the DFT [18]; the KS MOs do not define anything.

Very recently, an energy decomposition analysis based on the Interacting Quantum Atoms [26] (IQA), namely the Relative Interacting Atomic Energy [27] (RIAE), has been proposed to analyze the factors to controlling the activation energies; i.e., the changes in the IQA energies of the TSs with respect to the reference ground states. The RIAE analysis allows the decomposition of the KS energies obtained by the DFT calculations, allowing the

analysis of the electronic factors controlling the activation energies. The theoretical background of the RIAE analysis can be found in reference 27. Applying the RIAE analysis in three studies of polar DA reactions [27,28,29], it has been shown that the GEDT, which takes place from the nucleophile to the electrophile at polar TSs, is the main electronic factor responsible for the reduction of activation energies in polar reactions. These energy decomposition analyses have shown that while the nucleophile is destabilized by the loss of the electron density, the electrophile is stabilized. Since the stabilizing factor is greater than the destabilizing one, the GEDT phenomenon contributes to a decrease in the activation energy [29]. This finding supports Parr's proposal that the electrophilicity ω index is a measure of the stabilization of molecules when they receive an extra electron density [15].

Very recently, Bickelhaupt and Fernández have published an article entitled: "What defines electrophilicity in carbonyl compounds" [30]. In this article, the authors studied the nucleophilic attacks of cyanide anion **10** on a series of 4-substituted cyclohexanones **11a-f** and *p*-substituted benzaldehydes **12a-f** (see Scheme 2). These authors questioned the use of the electrophilicity ω index in the study of the reactivity of the carbonyl compounds. By using the Bickelhaupt's activation strain model [31] (ASM) and the Bickelhaupt's quantitative KS MO theory [32], the authors concluded that "electrophilicity is mainly determined by the electrostatic attractions between the carbonyl compound and the nucleophile (cyanide) along the entire reaction coordinate. Donor–acceptor frontier MO interactions, *on which the current rationale behind electrophilicity trends is based*, appear to have little or no significant influence on the reactivity of these carbonyl compounds." In the study of the addition of cyanide anion **10** to benzaldehydes **12a-f**, the authors found a linear correlation between the activation energies and the charges at the carbonyl carbon at the corresponding TSs.

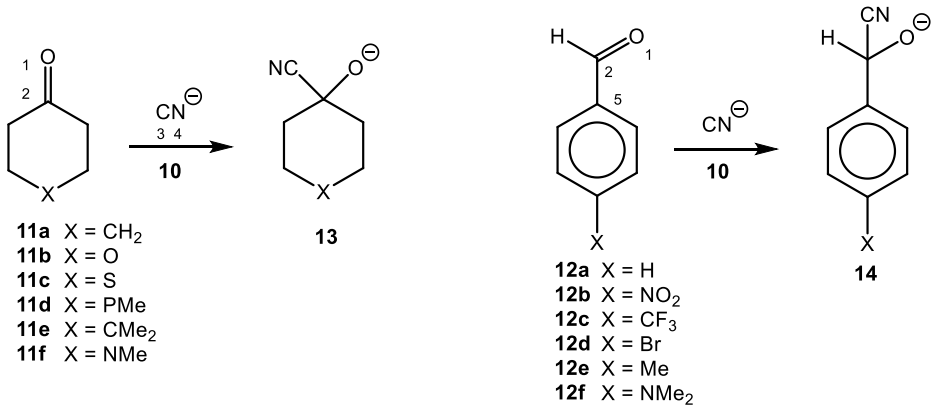

Scheme 2. Electrophilic additions of cyanide anion **10**
on the carbonyl carbon of cyclohexanones **11a-f** and benzaldehydes **12a-f**.

Some relevant issues regarding the ASM [31] and the KS MOs analyses applied in the Bickelhaupt and Fernández manuscripts should be commented on. First, to use the ASM within the DFT, Bickelhaupt proposed in 1999 the KS MO theory [32].

The DFT was established at the end of the 20th century, based on the theorems by Hohenberg and Kohn, as a new theory to study the electronic structure of matter [18]. In this quantum theory, the energy of a molecular system is a functional of the electron density ρ (see Equation 3). Unlike the MO theory [33], within DFT MOs do not exist. Unfortunately, similar to the quantum theory based on Schrödinger's equation [34], the resolution of the functional of the electron density ρ for a complex system is neither computationally feasible. As an approximation, the KS formalism [17] was introduced in analogy to the Hartree-Fock (HF) formalism [35]. Although the calculations performed within the KS formalism are similar to those performed in the HF approach, the KS wave function Ψ_{KS} is only used to obtain the electron density matrix, which is obtained by the square of the wave function Ψ_{KS}^2 [17]. In addition, only the occupied KS MOs are used to obtain the electron density matrix; the virtual KS MOs, which include the LUMO, are not used in the DFT calculations.

$$E[\rho] = F[\rho] + \int dr\, \rho(r) v(r) \tag{3}$$

Second, the electronic chemical potential μ [13] and the chemical hardness η [14] indices are obtained by the first and second derivatives of the DFT E[ρ] energies with respect to a number of electrons N to a constant external potential v(r). The mathematical approaches used in the derivation of E[ρ] equation give a series of equations that are functions of the I and A, which by using the Koopmans theorem [16] are approached by the frontier KS HOMO and LUMO energies as I by $-E_{HOMO}$ and A by $-E_{LUMO}$. Consequently, the electrophilicity ω index does not depend on "exclusively of the HOMO and LUMO energies" as these authors claim [30] since the values of KS HOMO and LUMO energies are used only in CDFT to approximate the molecular I and A energies. Note that the chemical electronic potential μ and the chemical hardness η could be obtained from I and A experimental data. In fact, in 2008, P. Pérez et al. reported a nucleophilicity N index obtained from the gas phase ionization potential I [36].

Consequently, the statement made in the conclusion of Bickelhaupt and Fernández's manuscript that "the donor-acceptor frontier molecular orbital interactions, on which the current rationale for electrophilicity trends is based" [30] is completely incoherent in DFT

since in this quantum chemistry theory MOs have no exit, and consequently, MO interactions, as proposed by the MO theory, can never be analyzed in DFT.

What is the electrophilicity? The electrophile/nucleophile concepts were proposed in 1930's to characterize the reagents involved in polar reactions [1]. As the feasibility of an organic reactions depends of its reaction rate, the electrophile/nucleophile were related to the kinetic of a reaction. The TS energies dependent on the several electronic factors that in many cases are difficult to analyze. However, many studies of polar reactions have shown that the GEDT taking place at the TSs is the main factor responsible for the reduction of activation energies in polar processes [10,11] (see Figure 1).

Very recently, the crucial role of the electron density transferred from the nucleophilic to the electrophilic species as the main factor reducing the activation energies has been established by a RIAE analysis of the series of polar DA reactions experimentally studied by Sauer (see Figure 1) [9,29]. This study has shown that the electronic stabilization of the electrophilic ethylene framework at the polar TSs is the main factor responsible for the acceleration found in these polar organic reactions, a behavior in complete agreement with the Parr's concept of the electrophilicity ω index [15,37]. Consequently, it is important to distinguish between the concept of electrophile, that is, the species that receive an amount of electron density in a polar process, and the Parr's electrophilicity ω index, that is, the CDFT index that quantitatively states the electrophilic character of an electrophile.

As previously mentioned, numerous manuscripts have shown the usefulness of the Parr's electrophilicity ω index for quantitatively characterizing the electrophilic character of an electrophile. Here, the two nucleophilic additions of cyanide anion **10** to carbonyl carbons given in Scheme 2 are studied within Molecular Electron Density Theory [38] (MEDT) to explore how the Parr's electrophilicity ω index is able to explain the chemical reactivity of this species.

Results and discussion

The present MEDT study has been organized into five sections: i) the first section contains an analysis of the electrophilicity ω indices of the cyclohexanones **11a-f** and benzaldehydes **12a-f**; ii) the second section conducts an electron localization function [39] (ELF) analysis of the electronic structure of the *p*-substituted benzaldehydes; iii) the third section explores the reaction paths associated with the nucleophilic addition of cyanide anion **10** to the cyclohexanone and benzaldehyde series; iv) the fourth section is focused on the ELF and quantum theory of Atoms in Molecules [40,41] (QTAIM) analyses of the evolution of the C–C bond formation at the TSs associated to the nucleophilic attacks of cyanide anion **10**

to cyclohexanone **11a** and benzaldehyde **12a**; and finally, v) the fifth section presents a RIAE analysis of the nucleophilic addition of cyanide anion **10** to benzaldehydes **12a,b,f**.

Analysis of the electrophilicity ω indices of the cyclohexanone **11a-f** and benzaldehyde **12a-f** series

First, the analysis of the electrophilicity ω indices of the cyclohexanones **11a-f** and benzaldehydes **12a-f** given in Scheme 2 was performed. The reactivity indices were calculated at the B3LYP/6-31G(d) computational level, which was employed to establish the electrophilicity scale [21,42]. The global reactivity indices, namely, the electronic chemical potential μ, chemical hardness η, global electrophilicity ω, and global nucleophilicity *N*, for the cyclohexanones **11a-f** and benzaldehydes **12a-f** are given in Table 2.

Table 2. B3LYP/6-31G(d) electronic chemical potential μ, chemical hardness η, electrophilicity ω, and nucleophilicity *N*, in eV, for cyclohexanones **11a-f** and benzaldehydes **12a-f**.

	X	μ	η	ω	*N*
12b	NO_2	–5.35	4.46	3.21	1.55
12c	CF_3	–4.77	5.07	2.25	1.81
12d	Br	–4.51	5.02	2.02	2.10
12a	H	–4.33	5.23	1.79	2.18
12e	Me	–4.22	5.24	1.70	2.28
16		–4.23	6.16	1.45	1.82
10		5.07	9.14	1.41	9.63
12f	NMe_2	–3.28	4.43	1.21	3.63
11b	O	–3.60	6.07	1.07	2.49
11c	S	–3.48	5.69	1.06	2.80
11d	PMe	–3.37	5.84	0.97	2.82
15		–3.47	6.34	0.95	2.48
11a	CH_2	–3.35	6.05	0.93	2.74
11e	CMe_2	–3.34	6.04	0.93	2.76
11f	NMe	–2.82	4.58	0.87	4.01

The electrophilicity ω indices of propan-2-one **15** and formaldehyde **16** are also analyzed as references to these carbonyl compounds. The electrophilicity ω indices of propan-2-one **15** and formaldehyde **16** are 0.95 and 1.45 eV, respectively. Consequently, these carbonyl compounds are classified as moderate electrophiles. Therefore, these molecules demand the acid or basic catalysis to experience nucleophilic additions. Note that the basic catalysis is achieved by the use of anion species such as the cyanide anion **10**, *N* = 9.63 eV (see Table 2), categorized as supernucleophiles species. The presence of the two

electron-releasing (ER) methyl groups in propan-2-one **15** markedly decreases the electrophilic character of this ketone with respect to that of formaldehyde **16**.

The electrophilicity ω index of cyclohexanone **11a**, 0.93 eV, is slightly lower than that of propan-2-one **15** (see Table 2). Consequently, it expected that cyclohexanone **11a**, will be poor reactive. The electrophilicity ω indices of the cyclohexanone derivatives **11b-f** are found in a narrow range between 0.87 – 1.07 eV. Therefore, a similar poor reactivity will be expected of this series of ketones in nucleophilic addition reactions. Analysis of the electrophilicity ω index of these ketones shows a relationship between the nature of the substitution X on the position 4 of cyclohexanone **11b-f** and the values of ω; thus, while tetrahydropyranone **11b** (X = O) is the most electrophilic species of this series, ω = 1.07 eV, 1-methylpiperidinone **11f** (X = NMe) is the less electrophilic one, ω = 0.87 eV. Therefore, this series of poor electrophilic ketones cannot be considered as presentative species of electrophilic molecules.

The electrophilicity ω index of benzaldehyde **12a**, 1.79 eV, is higher than that of formaldehyde **16** (see Table 2). The presence of the benzene ring in benzaldehyde **12a** increases its electrophilicity in $\Delta\omega$ = 0.34 eV with respect to that of formaldehyde **16**. Interestingly, the electrophilicity ω index of these *p*-substituted benzaldehydes is found in a wide range from 3.21 (**12b**, X = NO_2) to 1.21 (**12f**, X = NMe_2) eV. As can be seen, unlike in the series of cyclohexanones **11a-f**, the reactivity of these *p*-substituted benzaldehydes **12a-f** is strongly dependent on the substitution on the aromatic ring. Thus, while the presence of a strongly electron-withdrawing (EW) –NO_2 group increases the electrophilicity ω index of benzaldehyde **12a** in $\Delta\omega$ = 1.42 eV, the presence of the ER –NMe_2 group decreases it in $\Delta\omega$ = 0.58 eV.

The analysis of the electrophilicity ω index of cyclohexanone derivatives **11b-f** shows that these species, classified as moderate electrophiles, participate as electrophiles in polar reactions only under acid or basic catalysis. In addition, this series of 4-substituted cyclohexanones **11b-f** exhibit structural changes at the non-conjugated C-4 position relative to the carbonyl carbon of cyclohexanone **11a**. As a result, a poor response in the electrophilicity ω index and consequently in the reactivity would be expected.

Consequently, only the analysis of the electrophilicity ω index of the series of *p*-substitutes benzaldehydes **12a-f** can account for the participation of these species as electrophiles in polar reactions.

*ELF analysis of the electronic structure of the p-substituted benzaldehydes **12a,b,f**.*

The previous analysis of the electrophilicity ω index of the two series of carbonyl derivatives shows that only the *p*-substitution on the aromatic ring of benzaldehydes **12a-f** markedly affects its reactivity. The topological analysis of the ELF permits a quantitative characterization of the electron density distribution in a molecule [43], allowing the establishment of a correlation between its electronic structure and its reactivity. Thus, an ELF topological analysis of the electronic structures of benzaldehyde **12a** and the *p*-substituted benzaldehydes **12b** (X = NO_2) and **12f** (X = NMe_2) is carried out in order to show as the substitution affect the ground state electronic structures of these compounds. ELF basin attractor positions, together with the most relevant valence basin populations, are shown in Figure 3.

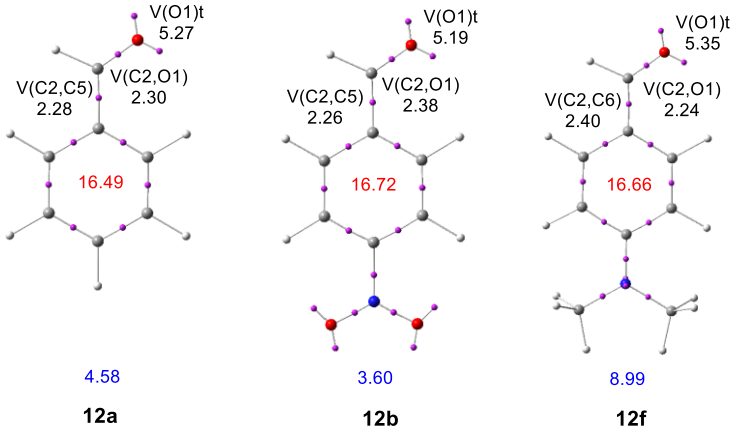

Fig. 3. ELF basin attractor positions and populations of the most relevant valence basins of benzaldehydes **12a**,**b**,**f**. The dipolar moments D, in debyes, are given in blue. The total electron density of the aromatic rings is given in red. Valence basin populations and ring electron density are given in average number of electrons, e.

ELF of benzaldehyde **12a** shows the presence of one V(C2,O1) disynaptic basin integrating 2.30 e, one V(C2,C5) disynaptic basin integrating 2.28 e, and two monosynaptic basins, V(O1) and V'(O1), integrating a total of 5.27 e. The six C–C bonding regions of the benzene aromatic ring are characterized by the presence of six V(C,C) disynaptic basins integrating a total of 16.49 e (see Figure 3).

The population of the V(C2,C4) disynaptic basin at the three benzaldehydes **12a**,**b**,**f** shows some delocalization between the carbonyl group and the benzene aromatic ring. On the other hand, the population of the V(C2,O1) disynaptic basins and that of the V(O1) and V'(O1) monosynaptic basins show a strong polarization of the electron density of the carbonyl C–O region toward the strong electronegative oxygen atom. Note that within the Lewis structure, the C–O region should be characterized as a populated single bond.

The presence of a strong EW $–NO_2$ group at the *p*-substituted benzaldehyde **12b** and a strong ER $–NMe_2$ group at the *p*-substituted benzaldehyde **12f** only modify slightly the population of the valence basins of benzaldehyde **12a** (see Figure 3). Thus, while EW $–NO_2$ group polarizes the electron density of the carbonyl C–O group towards the aromatic ring, the ER $–NMe_2$ group polarizes the corresponding electron density towards the carbonyl oxygen atom.

The effects of the benzene substitution on the polarization of the carbonyl group are displayed in the dipolar moment D of these molecules; the strong polarization of the electron density at the *p*-NMe_2-benzaldehyde **12f** causes an increase of the dipole moment of this species with respect to that in the other two compounds (see Figure 3). The electron density in the C=O bonding region of these three benzaldehydes is again the electrophilicity ω index showed by them. Note that the most electrophilic species **12b** presents the high V(C2,O1) populations.

Study of the nucleophilic addition of cyanide anion to the cyclohexanone and benzaldehyde series

Next, the potential energy surface (PES) associated with the nucleophilic addition of cyanide anion **10** to the cyclohexanones **10a,b,f** and benzaldehydes **12a,b,c,e,f** to yield the corresponding tetrahedral adduct intermediates was analyzed.

Study of the nucleophilic addition of cyanide anion **10** to the cyclohexanones **10a,b,f**.

Due to the similar reactivity expected for the nucleophilic addition of cyanide anion **10** to the cyclohexanone series given in Table 2, only the nucleophilic addition to cyclohexanone **11a** and the cyclohexanone derivatives **11b** (X=O) and **11f** (X=NMe) were studied (see Scheme 3). For comparison, the nucleophilic attack of cyanide anion **10** to propan-2-one **15** was also studied. The total and relative energies are given in Table 3.

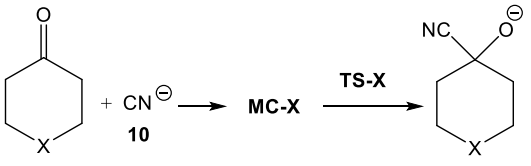

Scheme 3. Electrophilic addition of cyanide anion **10** on the carbonyl carbon of cyclohexanones **11a**,**b**,**f**.

Along the approach of the cyanide anion **10** to these carbonyl compounds a series of weak molecular complexes (MCs) are found on the PES. They are only between 0.8 and 1.1 kcal·mol^{-1} more stable than the separated reagents. Therefore, they have no relevance for PES. The nucleophilic attack of cyanide anion **10** on the carbonyl carbon atom of propan-2-one **15** presents an activation energy of 12.9 kcal·mol^{-1}, formation of the corresponding tetrahedral adduct intermediate **AD-15** is endothermic by 6.13 kcal·mol^{-1}. A similar energy result is obtained for the addition of the cyanide anion **10** to cyclohexanone **11a**.

Table 3**.** Total, in au, and relative, in kcal·mol^{-1}, energies of the stationary points involved in the step of the nucleophilic attack of cyanide anion **10** on the carbonyl carbon of propan-2-one **15** and cyclohexanones **11a**,**b**,**f**.

	E	ΔE
propan-2-one **15**	–193.156742	
MC-15	–286.111573	–0.84
TS-15	–286.089606	12.94
AD-15	–286.100456	6.13
11a (X = CH_2)	–309.889201	
MC-11a	–402.844099	–0.88
TS-11a	–402.823814	11.85
AD-11a	–402.835564	4.47
11b (X = O)	–345.780943	
MC-11b	–438.736242	–1.14
TS-11b	–438.718566	9.96
AD-11b	-438.731222	2.02
11f (X = NMe)	–365.224374	
MC-11f	–458.179056	–0.75
TS-11f	–458.160703	10.77
AD-11f	–458.172739	3.22
CN^- **10**	–92.9534898	

The activation energy associated with this addition is only 1.1 kcal·mol^{-1}, lesser than that associated with propan-2-one **15**. On the other hand, the activation energies associated with the nucleophilic attacks to 4-substituted cyclohexanones **11b** (X = O) and **11f** (X = NMe) are 2.0 and 1.0 kcal·mol^{-1}, respectively, lower in energy than cyclohexanone **11a**. A similar trend in the endothermic character of the formation of the corresponding tetrahedral adduct intermediates is found. The lesser electrophilic cyclohexanone **11f** presents a lower activation energy than cyclohexanone **11a**. The different activation energies, which show the same trend that the thermodynamic formation of the tetrahedral adduct intermediates, may be due to some weak electronic interactions that are not easy to analyze.

The geometries of the TSs associated with the nucleophilic attack of cyanide anion **10** on the carbonyl carbon atom of propan-2-one **15** and cyclohexanone **11a** are given in Figure 4. The two main parameters of these TSs are the C2–C3 distance and the C3–C2–O1 angle. The C2–C3 distance at these TSs are 1.980 (**TS-15**) and 2.004 (**TS-11a**) Å, while the C3–C2–O1 angles are 107.5 (**TS-15)** and 106.2 (**TS-11a**) degrees. The C2–C3 distances at the TSs associated with the nucleophilic attacks of cyanide anion **10** to cyclohexanones **11b** (X = O) and **11f** (X = NMe) are very similar, 2.008 and 2.001 Å, respectively.

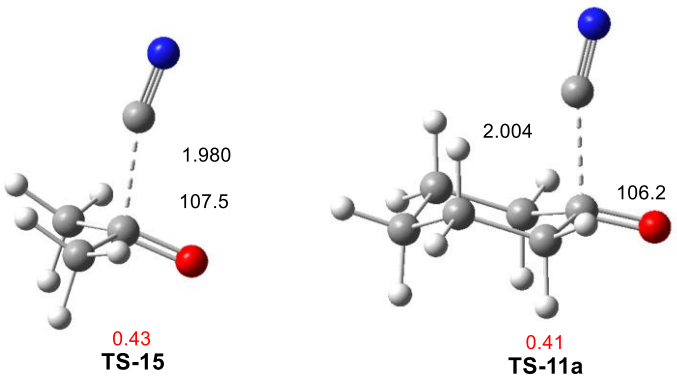

Fig. 4. Geometries of the TSs associated with the nucleophilic attack of cyanide anion **10** on the carbonyl carbon of propan-2-ona **15**, **TS-15**, and cyclohexanone **11a**, **TS-11a**. The GEDT is given in red. Distances are given in Angstroms Å, while angles are given in degrees.

Finally, the GEDT at these TSs, which shows the polar character of an organic reaction, was computed [8]. The corresponding GEDT values are given in Figure 4. The high GEDT computed at these TSs, *ca.* 0.42 e, points out to the high polar character of these nucleophilic addition reactions, resulting from the supernucleophilic character of cyanide anion **10**, and not to the poor electrophilic character of these carbonyl compounds (see Table 2).

Study of the nucleophilic addition of cyanide anion **10** to benzaldehydes **12a,b,c,e,f**.

For the nucleophilic addition reactions of cyanide anion **10** to benzaldehydes **12a-f** given in Scheme 2, five reactions were studied. They include the attack of cyanide anion **10** to benzaldehyde **12a**, and the attacks to the *p*-substituted benzaldehydes **12b** and **12c** having the EW $-NO_2$ and $-CF_3$ groups, respectively, and to the *p*-substituted benzaldehydes **12e** and **12f** having the ER $-CH_3$ and $-N(CH_3)_2$ groups (see Scheme 4). The total and relative energies are given in Table 4.

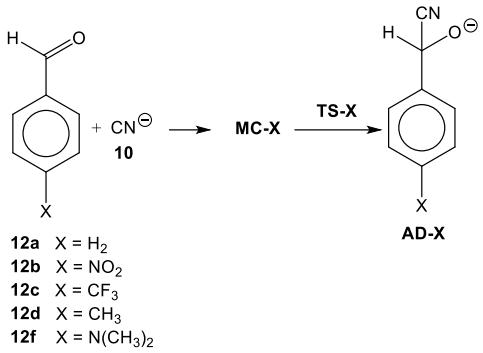

Scheme 4. Electrophilic addition of cyanide anion **10** on the carbonyl carbon of benzaldehydes **12a,b,c,d,f**.

Table 4. Total, in au, and relative, in kcal·mol^{-1}, energies of the stationary points involved in the step of the nucleophilic attack of cyanide anion **10** on the carbonyl carbon of benzaldehydes **12a**,**b,c,e,f**.

	E	ΔE
12b (X = NO_2)	–550.044495	
MC-12b	–643.000738	–1.73
TS-12b	–642.987294	6.71
AD-12b	–643.000203	–1.39
12c (X = CF_3)	–682.605589	
MC-12c	–775.561742	–1.67
TS-12c	–775.546222	8.07
AD-12c	–775.558812	0.17
12a (X = H)	–345.547859	
MC-12a	–438.502900	–0.97
TS-12a	–438.484828	10.37
AD-12a	–438.496786	2.86
12e (X = Me)	–384.865040	
MC-12e	–477.819903	–0.86
TS-12e	–477.800580	11.26
AD-12e	–477.812317	3.9
12f (X = NMe_2)	–479.519337	
MC-12f	–572.474554	–1.08
TS-12f	-572.449452	14.67
AD-12f	-572.460477	7.75

Similar to the addition to cyclohexanone **11a**, a series of MCs along the approach of cyanide anion **10** to these benzaldehyde derivatives are found. They are only between 0.9 and 1.8 kcal·mol^{-1} more stable than the separated reagents (see Table 4). The activation energies associated with these nucleophilic attacks range from 6.7 (**12b** (X = NO_2)) to 14.7 (**12f** (X = NMe_2)) kcal·mol^{-1}, while the endothermic character of formation of the

corresponding tetrahedral adduct intermediates range from 0.17 (**12c** (X = CF_3)) to 7.75 a (**12f** (X = NMe_2)) kcal·mol^{-1}; i.e., the *p*-substitution on the benzene ring has a marked incidence in the kinetics and in the thermodynamics. If the addition to benzaldehyde **12a** is taken as the reaction reference, the presence of a strong EW $-NO_2$ substituent at **12b** clearly reduces the activation energy to 6.7 kcal·mol^{-1}, while the presence of a strong ER $-N(CH_3)_3$ substituent at **12f** increases it to 14.7 kcal·mol^{-1}.

As shown in Figure 5, a very good logarithmic correlation between the electrophilicity ω index of benzaldehydes **12a**,**b,c,e,f** and the activation energies associated with the nucleophilic attack of the cyanide anion **10** on these species can be established, R^2 = 0.95. This plot shows the narrow correlation between the values of the electrophilicity ω index and the variations of activation energies in these polar reactions.

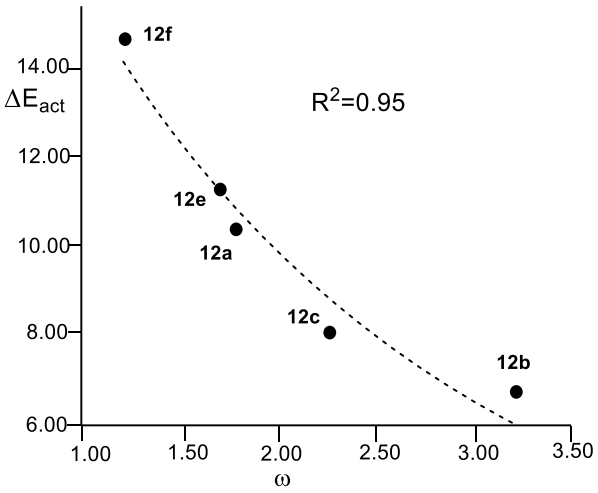

Fig. 5. Plot of the activation energies associated with the nucleophilic attack of cyanide anion **10** to benzaldehydes **12a,b,c,e,f**, ΔE_{act} in kcal·mol^{-1}, versus the electrophilicity ω index, in eV, of benzaldehydes **12a,b,c,e,f**.

The geometries of the TSs associated with the nucleophilic attack of cyanide anion **10** on the carbonyl carbon atom of benzaldehydes **12a,b,f** are given in Figure 6. The C2–C3 distance at these TSs, 2.022 (**TS-12b**), 1.995 (**TS-12a**) and 1.970 (**TS-12f**) Å are closer to that associated with the attached to cyclohexanone **11a** (see Figure 4). These data show a relationship between these distances and the corresponding activation energies, in agreement with the Hammond's postulate [44]; the lower the activation energy, earlier the TS.

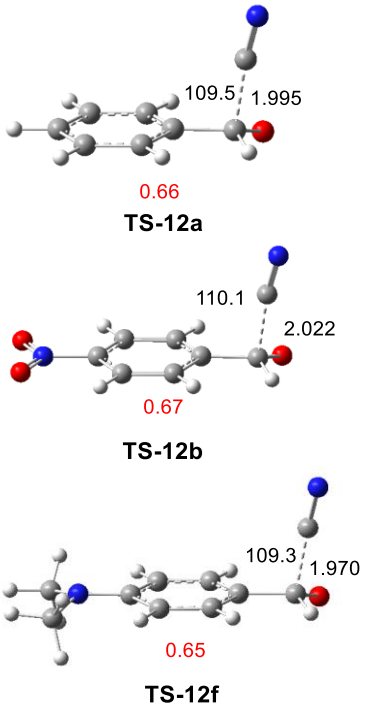

Fig. 6. geometries of the TSs associated to the nucleophilic attack of cyanide anion **10** on the carbonyl carbon of benzaldehydes **12a,b,f**. The GEDT values at the TSs are given in red. Distances are given in Angstroms Å, while angles are given in degrees. The GEDT is given in average number of electrons, e.

Finally, the GEDT at the TSs was computed. The corresponding GEDT values are given in Figure 6. The high GEDT computed at these TSs, *ca.* 0.65 e, points out to the high polar character of this nucleophilic addition reactions. These values are higher than those computed at the TSs of the addition to cyclohexanone **11a** (see Figure 4), in agreement with the higher electrophilic character of benzaldehydes than cyclohexanones (see Table 2). Newly, the high polar character of these TSs is a consequence of the supernucleophilic character of the anion cyanide **10**.

In Figure 7, a very good linear correlation between the GEDT computed to the TSs and the activation energies associated with the nucleophilic attack of the cyanide anion **10** to benzaldehydes **12a,b,c,e,f** can be established, R^2 = 0.97. This plot shows the dependence of the activation energy of polar organic reaction of the GEDT taking place at the TSs [29]; the more GEDT at the TSs, i.e., the more polar the reaction, the faster the reaction (see Figure 1).

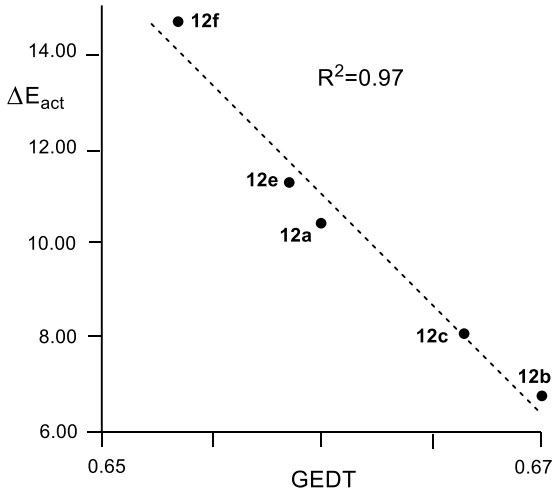

Fig. 7. Plot of the activation energies associated with the nucleophilic attack of cyanide anion **10** to benzaldehydes **12a,b,c,e,f** (ΔE_{act}, in kcal·mol^{-1}) versus the GEDT, in average number of electrons e, computed at the TSs.

ELF and QTAIM analyses of the evolution of the C–C bond formation at the TSs associated to the nucleophilic attacks of cyanide anion **10** to cyclohexanone **11a** and benzaldehyde **12a**.

In order to understand the evolution of the C–C bond formation at the TSs associated to the nucleophilic attacks of cyanide anion **10** to cyclohexanone **11a** and benzaldehyde **12a** an ELF and QTAIM topological analysis of **TS-11a** and **TS-12a** was performed. ELF basin attractor positions, together with the most relevant valence basin populations at the two TSs are shown in Figure 8.

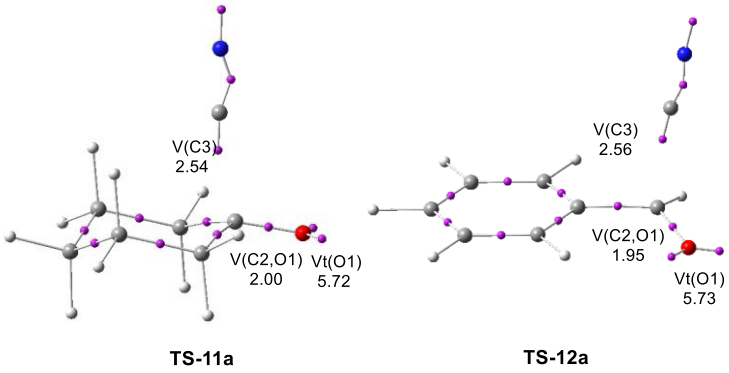

Fig. 8. ELF basin attractor positions and populations of the most relevant valence basins of **TS-11a** and **TS-12a**. Valence basin populations are given in average number of electrons, e.

The analysis of the ELF in both TSs shows a great similarity between them. They show the presence of a V(C3) monosynaptic basin integrating 2.5 e at the cyanide carbon atom. The absence of any V(C2,C3) disynaptic basin between the cyanide carbon atom and the carbonyl one indicates that at both TSs the formation of the new C2–C3 single bond has not

yet started. A comparison of the electron density at the carbonyl group at benzaldehyde **11a** (see Figure 3) and that at **TS-12a** shows that along the approach of the cyanide anion **10** to the carbonyl carbon atom, a strong polarization of the electron density toward the carbonyl oxygen atom takes place.

A comparative QTAIM analysis of the C2···C3 interacting regions in **TS-11a** and **TS-12a** shows a high degree of electronic similarity between the two TSs (see Figure 9). The critical points (CPs) (3,-1) associated with the C2···C3 interacting regions at both TSs present the same electron density ρ = 0.08 e (see Table 5). The Laplacian $\nabla^2\rho$(r) at these CPs show positive values, indicating the absence of any covalent interaction, $\nabla^2\rho$(r) = 0.03. The calculated |V(r)|/G(r) values at these CPs, 1.77 (**TS-11a**) and 1.73 (**TS-12a**) indicate that, according to the Espinosa criteria [45], the corresponding C2···C3 interactions have a non-covalent nature with somewhat covalent character

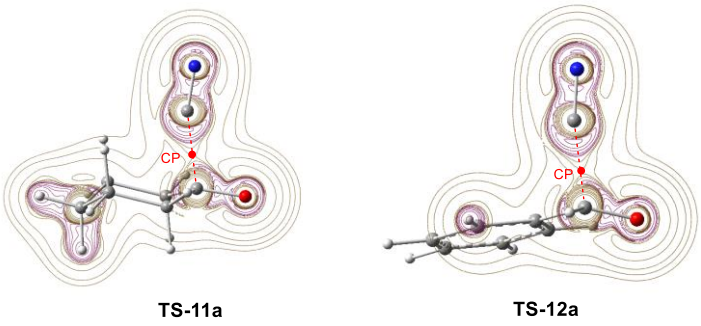

Fig. 9. Representations of ωB97X-D/6-311+G(d,p) contour line maps of the Laplacian $\nabla^2\rho$(r) of the electron density of **TS-11a** and **TS-12a**. The CPs (3,-1) CP and the bond path associated with the C2···C3 interacting region are marked in red.

Table 5. ωB97X-D/6-311+G(d,p) QTAIM parameters, in atomic units a.u., of the (3,-1) CPs at **TS-11a** and **TS-12a**.

	TS-11a	**TS-12a**
Density	0.0826	0.0829
Laplacian	0.0306	0.0381
G(r)	0.0339	0.0361
K(r)	0.0262	0.0266
V(r)	–0.0601	–0.0627
V(r)|/G(r)	1.7741	1.7363

RIAE analysis of the nucleophilic addition of cyanide anion **10** to benzaldehydes **12a,b,f**.

Finally, to determine the electronic effects responsible for the activation energies of the nucleophilic addition of cyanide anion **10** to benzaldehydes **12a-f**, a RIAE analysis [27] on the gas-phase TSs associated with the nucleophilic addition of cyanide **10** anion to benzaldehydes **12a** (X=H), **12b** (X=NO_2) and **12f** (X=NMe_2) was performed. The

nucleophilic addition reaction to formaldehyde **16** as the reaction reference is also studied. The M06-2X/6-311+G(d,p) ξE^X_{total} total, ξE^X_{intra} intra-atomic and ξE^X_{inter} interatomic energies of the benzaldehyde (CHO) and cyanide anion (CNA) frameworks of the TSs with respect to the MCs are given in Table 6.

Analysis of the ξE^X_{total} energies of the two frameworks in the nucleophilic addition of cyanide **10** anion to formaldehyde **16** shows that while the nucleophilic CNA framework is destabilized at **TS-16**, ξE^{CNA}_{total} = 8.34 kcal·mol^{-1}, the electrophilic CHO one is stabilized, ξE^{CHO}_{total} = −3.78 kcal·mol^{-1}. Analysis of the ξE^X_{intra} intra-atomic and ξE^X_{inter} interatomic energies at the two fragments indicates that while the intramolecular interactions at the CHO framework is the more stabilizing factor, ξE^{CHO}_{intra}= −9.4 kcal·mol^{-1}, the intramolecular interactions at the CNA framework is the more destabilizing factor, ξE^{CNA}_{intra}= 35.87 kcal·mol^{-1}.

Analysis of the ξE^X_{total} total energies of the TS associated with the nucleophilic addition of cyanide anion **10** to benzaldehyde **12a** (X = H) shows a similar trend to that associated with the addition to formaldehyde **16**. While the ξE^X_{total} total energies associated with CHO framework are stabilizing, ξE^{CHO}_{total} = −2.40 kcal·mol^{-1}, those associated with the CNA one as destabilizing, ξE^{CNA}_{total} = 10.46 kcal·mol^{-1}. In this reaction, the ξE^X_{inter} interatomic energies associated with the CHO framework of **TS-12** are the more favorable, ξE^X_{inter} = −19.13 kcal·mol^{-1}.

Table 6. M06-2X/6-311+G(d,p) gas-phase ξE^X_{total} total, ξE^X_{intra} intra-atomic and ξE^X_{inter} interatomic energies, in kcal·mol^{-1}, of the benzaldehyde CHO and cyanide anion CNA frameworks at the TSs with respect to those at the MCs. The sum of the of the ξE^X_{total} energies of the two frameworks, i.e., $\xi E^{CHO+CNA}_{total}$, yields the RIAE activation energies.

	f(X)	ξE^X_{intra}	ξE^X_{inter}	ξE^X_{total}	$\xi E^{CHO+CNA}_{total}$
TS-16	CHO	–9.41	5.63	–3.78	4.56
	CNA	35.87	–27.53	8.34	
TS-12a (X=H)	CHO	16.73	–19.13	–2.40	8.06
	CNA	25.17	–14.72	10.46	
TS-12b (X=NO_2)	CHO	22.80	–29.85	–7.05	4.70
	CNA	–4.60	16.35	11.75	
TS-12f (X=NMe_2)	CHO	–64.48	67.25	2.77	15.20
	CNA	13.77	–1.35	12.43	

The inclusion of a strong EW $-NO_2$ group in the aromatic ring of benzaldehyde causes a marked stabilization of the CHO framework of **TS-12b** (X = NO_2), ξE^{CHO}_{total}= −7.05 kcal·mol^{-1}, while the CNA one is destabilized ξE^{CNA}_{total}= 11.75 kcal·mol^{-1}. The high stabilization of the CHO framework resulting from the high GEDT decreases the RIAE activation energy with respect to that of **TS-12a** (X = H) by 3.36 kcal·mol^{-1}. A detailed analysis of the energies

given in Table 6 indicates that the ξE_{inter}^{CHO} interatomic energies associated with the benzaldehyde CHO framework, –29.85 kcal·mol^{-1}, are the more stabilizing factors at the most favorable **TS-12b**, while those associated with the cyanide anion CNA framework are destabilizing, ξE_{inter}^{CNA} = 16.35 kcal·mol^{-1}. Analysis of the IQA interatomic energies contributing to the ξE_{inter}^{CHO} interatomic energies shows that the stabilization of the carbonyl C2 carbon atom, ξE_{inter}^{C2}= –41.52 kcal·mol^{-1}, is the main factor contributing to that stabilization.

The inclusion of a strong ER –NMe_2 group in the aromatic ring of benzaldehyde causes a marked destabilization of the two interacting CHO and CNA frameworks of **TS-12f** (X = NMe_2), ξE_{total}^{X} = 2.77 (CHO) and 12.43 (CNA) kcal·mol^{-1}. Although the ξE_{intra}^{CHO} intra-atomic energies are strongly stabilizing, –64.48 kcal·mol^{-1}, the ξE_{inter}^{CHO} interatomic energies are more strongly destabilizing, 67.25 kcal·mol^{-1}. As a consequence, the RIAE activation energies arises to 15.20 kcal·mol^{-1}.

As expected in polar reactions, while the ξE_{total}^{CNA} total energies associated with the nucleophilic cyanide anion **10** are positive and unfavorable, the ξE_{total}^{CHO} total energies associated with the electrophilic aldehydes **16** and **12a,b** are negative and favorable (see Table 6) [29]. This result is a consequence of the GEDT taking place at the polar TSs which stabilize the electrophilic CHO frameworks, a behavior anticipated by analysis of the Parr's electrophilicity ω index [15,37].

Table 7. IQA E_{inter}^{C2C3} interatomic energies, in a.u., between the C2 and C3 interacting carbons at the TSs.

	E_{inter}^{C2C3}	V_{en}^{C2C3}	V_{ne}^{C2C3}	V_{ee}^{C2C3}	V_{nn}^{C2C3}
TS-16	0.0253	–7.9136	–8.6634	7.1362	9.4661
TS-12a	0.0350	–7.6286	–8.4010	6.9139	9.1507
TS-12b	0.0404	–7.1886	–7.9842	6.5784	8.6348
TS-12f	0.0329	–7.7499	–8.5156	7.0061	9.2923

In order to understand the electronic interactions taking place between the pair of C2 and C3 interacting carbon atoms at the aforementioned TSs, an IQA analysis of the V_{inter}(A,B) interatomic energies between the C2 and C3 carbons at the four TSs was performed (see Table 7). Three interesting conclusions can be drawn from a detailed energy analysis of the data given in Table 7: i) in the four TSs, the sum of the V_{en}^{C2C3} and V_{ne}^{C2C3} attractive energies is lower than the V_{ee}^{C2C3} and V_{nn}^{C2C3} repulsive ones by between 15.89 (**TS-16**) and 25.26 (**TS-12b**) kcal·mol^{-1}; ii) the repulsive nuclei-nuclei V_{nn}^{C2C3} interatomic interactions are the main factor responsible of these unfavorable interactions, and iii) these

repulsive interactions decrease in the order **TS-12f** > **TS-12a** > **TS-12b**, as the C2–C3 distance increase.

Consequently, this RIAE analysis rejects the main conclusions of Bickelhaupt and Fernández's manuscript obtained through the ASM analysis that "electrophilicity is mainly determined by the electrostatic attractions between the carbonyl compound and the nucleophile (cyanide) along the entire reaction coordinate" [30], since the increase of the favorable ξE_{inter}^{CHO} interatomic energies associated with the electrophilic benzaldehyde CHO framework, resulting from the GEDT taking place at the polar TSs, are the main factor responsible for the acceleration of these polar reactions. In addition, the IQA analysis of the C2 and C3 electrostatic interactions taking place at the TSs of these nucleophilic additions indicates that they are repulsive and consequently unfavorable.

Computational Details

This MEDT study has been carried out by performing quantum chemical calculations within DFT. The ωB97X-D functional [46], together with the standard 6-311+G(d,p) basis set [35], which includes diffuses and d-type polarization for second-row elements and p-type polarization functions for hydrogens, were used throughout this MEDT study. The TSs were characterized by the presence of only one imaginary frequency. The Berny method was used in optimizations [47,48]. The intrinsic reaction coordinate [49] (IRC) calculations were performed to establish the unique connection given between the TSs and the corresponding minima [50,51]. Solvent effects were considered by full optimization of the gas phase structures at the same computational level using the polarizable continuum model [52,53] (PCM) in the framework of the self-consistent reaction field [54-56] (SCRF), and water as solvent. The GEDT [8] values were computed using the equation GEDT(f) = Σq_f, where q are the natural charges [57,58] of the atoms belonging to one of the two frameworks (f) at the TS geometries. Reactivity indices [13,25] were calculated using the equations in reference [25].

The Gaussian 16 suite of programs [59] was used to perform the calculations. ELF analyses of the ωB97X-D /6-311+G(d,p) monodeterminantal wavefunctions were done by using the TopMod [60] package with a cubical grid of step size of 0.1 Bohr. The Bader's QTAIM [32,33] analyses were conducted using Multiwfn 3.7 software packages [61]. Molecular geometries and ELF basin attractors were visualized by using the GaussView program [62].

The IQA analysis was performed with the AIMAll package [63] using the corresponding

M06-2X/6-311+G(d,p) monodeterminantal pseudo-wavefunctions. Note that the AIMAll package only allows the use of the B3LYP and the M06-2X functionals.

Conclusions

In 1933, Ingold introduced the terms electrophile and nucleophile to refer to the species involved in polar organic reactions [1]. In 1999, Parr proposed the electrophilicity ω index into the CDFT as a measure of the electronic stabilization of a molecule when it acquires an additional amount of electron density [15]. Since 1999, a strong correlation has been established between the GEDT occurring at the TSs of polar reactions and the activation energies. Finally, in 2024, a RIAE analysis of polar DA reactions experimentally studied by Sustman in 1964 [9] has allowed to establish the decisive role of the electron density transferred to the electrophilic framework in reducing the activation energies of polar reactions [27-29], thus supporting the Parr's electrophilicity ω index as a quantitative measure of the electrophilic character of a species. [15,37].

Recently, the electrophilicity ω index in the study of a series of 4-subtituted cyclohexanones has been questioned in a manuscript entitled *What defines electrophilicity in carbonyl compounds* [29]. The present MEDT study shows that 4-subtituted cyclohexanones with ω < 1.07 eV are poor electrophiles that undergo nucleophilic addition reactions only with supernucleophiles such as the cyanide anion **10**, in the called basic catalysis. Consequently, 4-subtituted cyclohexanones are not adequate models of electrophilic species. In addition, the 4-position of cyclohexanone **11a** is not conjugated to the carbonyl group. Therefore, the electronic behavior of the substitution in the non-conjugated C4 carbon of cyclohexanone **11a** has little effect on both the electrophilicity ω index and the activation energies.

A different behavior is found in the nucleophilic addition of cyanide anion **10** to *p*-substituted benzaldehydes, since the *para* position is conjugated to the carbonyl group. Here, both the electrophilic ω index as well as the activation energies associated with the nucleophilic attack on the carbonyl group account for the electronic effects of the groups present in the *para* position of the benzaldehyde **12a**.

The present MEDT study rejects the main conclusions of Bickelhaupt and Fernández manuscript that "*electrophilicity is mainly determined by the electrostatic attractions between the carbonyl compound and the nucleophile (cyanide) along the entire reaction coordinate*" [30]. The RIAE analysis of these nucleophilic additions suggests that the increase of the favorable ξE_{inter}^{CHO} interatomic energies associated with the electrophilic benzaldehyde CHO

framework, resulting from the GEDT taking place at the polar TSs, is the main factor responsible for the acceleration of these polar reactions [29]. Finally, the IQA analysis between the two interacting carbon atoms at the TSs, i.e. the carbonyl carbon atom and the cyanide carbon atom, indicates that the corresponding electrostatic interactions are repulsive.

This study emphasizes the relevance of Parr's electrophilicity ω index as a quantitative measure of the electrophilic character of the species involved in a polar reaction.

References

[1] Ingold, C.K.; Significance of Tautomerism and of the Reactions of Aromatic Compounds in the Electronic Theory of Organic Reactions. *J. Chem. Soc.* **1933**, 1120-1127. DOI: 10.1039/JR9330001120

[2] Lapworth, A.; Replaceability of Halogen Atoms by Hydrogen Atoms: A General Rule. *Nature* **1925**, 115-625.

[3] Mayr, H.; Patz, M.; scales of Nucleophilicity and Electrophilicity: A System for Ordering Polar Organic and Organometallic Reactions. *Angew. Chem., Int. Ed. Engl.* **1994**, 33, 938-957. DOI: 10.1002/anie.199409381

[4] Mayr, H.; Bug, T.; Gotta, M. F.; Hering, N.; Irrgang, B.; Janker, B.; Kempf, B.; Loos, R.; Ofial, A. R.; Remennikov, G.; Schimmel, H.; Reference Scales for the Characterization of Cationic Electrophiles and Neutral Nucleophiles. *J. Am. Chem. Soc.* **2001**, 123, 9500-9512. DOI: 10.1021/ja010890y

[5] Lucius, R.; Loos, R.; Mayr, H.; Combinations: Key to a General Concept of Polar Organic Reactivity. *Angew. Chem., Int. Ed.* **2002**, 41, 91-95. DOI: 10.1002/1521-3773(20020104)41:1<91::AID-ANIE91>3.0.CO;2-P

[6] Phan, T. B.; Breugst, M.; Mayr, H.; Towards a General Scale of Nucleophilicity?. *Angew. Chem., Int. Ed.* **2006**, 45, 3869-3874.

[7] Domingo, L.R.; Arnó, M.; Andrés, J ; Influence of reactant polarity on the course of the inverse-electron-demand Diels-Alder reaction. A DFT study of regio- and stereoselectivity, presence of Lewis acid catalyst, and inclusion of solvent effects in the reaction between nitroethene and substituted ethenes, *J. Org. Chem.* **1999**, 64, 5867–5875. DOI: 10.1021/jo990331y

[8] Domingo, L.R.; A new C-C bond formation model based on the quantum chemical topology of electron density. *RSC Adv.* **2014**, 4, 32415–32428. DOI: https://doi.org/10.1039/C4RA04280H

[9] Sauer, J.; Wiest, H.; Mielert, A.; Eine Studie der Diels-Alder-Reaktion, I. Die Reaktivität von Dienophilen gegenüber Cyclopentadien und 9.10-Dimethyl-anthracen. *Chem. Ber.* **1964**, 97, 3183–3207. DOI: 10.1002/cber.19640971129

[10] Domingo, L. R.; Aurell, M. J.; Pérez, P.; Contreras, R.; Origin of the synchronicity on the transition structures of polar Diels-Alder reactions. Are these reactions [4+2] processes?. *J. Org. Chem.* **2003**, 68, 3884–3890. DOI: 10.1021/jo020714n

[11] Domingo, L.R.; Sáez, J.A.; Understanding the mechanism of polar Diels-Alder reactions, *Org. Biomol. Chem.*, **2009**, 7, 3576–3583. DOI: 10.1039/B909611F

[12] Parr, R. G.; Yang, W.; Density-functional theory of the electronic structure of molecules. *Annu. Rev. Phys. Chem.* **1995**, 46, 701-728. DOI: 10.1146/annurev.pc.46.100195.003413

[13] Parr, R.G.; Yang,W. Density Functional Theory of Atoms and Molecules; Oxford University Press: New York, NY, USA, 1989.

[14] Parr, R. G.; Pearson, R.G.; Absolute hardness: companion parameter to absolute electronegativity. *J. Am. Chem. Soc.* **1983**, 105, 7512-7516.

[15] Parr, R. G.; von Szentpaly, L.; Liu, S.; Electrophilicity index. *J. Am. Chem. Soc.* **1999**, *121*, 1922 -1924. DOI: 10.1021/ja983494x

[16] Koopmans, T.; Über die Zuordnung von Wellenfunktionen und Eigenwerten zu den Einzelnen Elektronen Eines Atoms. *Physica* **1933**, *1*, 104-113. DOI: 10.1016/S0031-8914(34)90011-2

[17] Kohn, W.; Sham, L. J.; Self-consistent equations including exchange and correlation effects. *Phys. Rev. B* **1965**, *140*, A1133-A1138. DOI: 10.1103/PhysRev.140.A1133

[18] Hohenberg, P.; Kohn, W.; Inhomogeneous electron gas Kohn, W. *Physical Review* **1964**, 136, B864 -B871. DOI: 10.1103/PhysRev.136.B864

[19] Pérez, P.; Domingo, L.R.; Aizman, A.; Contreras, R.; The Electrophilicity Index in Organic Chemistry, In Theoretical Aspects of Chemical Reactivity. Elsevier. New York. 19, **2007**, pp 139-201. DOI: 10.1016/S1380-7323(07)80010-0

[20] Domingo, L. R.; Ríos-Gutiérrez, M.; In Application of Reactivity Indices in the Study of Polar Diels–Alder Reactions. Conceptual Density Functional Theory: Towards a New Chemical Reactivity Theory, Ed. Shubin Liu. WILEY-VCH GmbH. **2022**, Vol. 2, pp, 481–502. DOI: 10.1002/9783527829941.ch24

[21] Domingo, L. R.; Aurell, M. J.; Pérez, P.; Contreras, R.; Quantitative characterization of the global electrophilicity power of common diene/dienophile pairs in Diels-Alder reactions. *Tetrahedron* **2002**, *58*, 4417-4423. DOI: 10.1016/S0040-4020(02)00410-6

[22] Domingo, L.R.: Ríos-Gutiérrez, M.; Pérez, P.; Why is Phenyl Azide so Unreactive in [3+2] Cycloaddition Reactions? Demystifying Sustmann's Paradigmatic Parabola. *Org. Chem. Front.* **2023**, 10, 5579-5591. DOI: 10.1039/D3QO00811H

[23] Domingo, L.R.; Pérez, P.; Sáez, J.A.; Understanding the local reactivity in polar organic reactions through electrophilic and nucleophilic Parr functions. *RSC Adv.* **2013**, 3, 1486-1494. DOI: 10.1039/C2RA22886F

[24] Domingo, L.R.; Chamorro, E.; Pérez, P.; Understanding the Reactivity of Captodative Ethylenes in Polar Cycloaddition Reactions. A Theoretical Study. *J. Org. Chem.* **2008**, 73, 4615-4624. DOI: 10.1021/jo800572a

[25] Domingo, L.R.; Ríos-Gutiérrez, M.; Pérez, P.; Applications of the Conceptual Density Functional Theory Indices to Organic Chemistry Reactivity. *Molecules* **2016**, 21, 748. DOI: 10.3390/molecules21060748

[26] Blanco, M. A.; Martín Pendás, A.; Francisco, E.; Interacting Quantum Atoms: A Correlated Energy Decomposition Scheme Based on the Quantum Theory of Atoms in Molecules, *J. Chem. Theory Comput.* **2005**, 1, 1096–1109. DOI: 10.1021/ct0501093

[27] Domingo, L.R.: Ríos-Gutiérrez, M.; Pérez, P.; Understanding the Electronic Effects of Lewis Acid Catalysts in Accelerating Polar Diels-Alder Reactions. *J. Org. Chem.* **2024**. DOI: 10.1021/acs.joc.4c01297.

[28] Domingo, L.R.; Pérez, P.; Ríos-Gutiérrez, M.; Aurell, M.J.; A Molecular Electron Density Theory Study of Hydrogen Bond Catalysed Polar Diels–Alder Reactions of α,β-unsaturated Carbonyl Compounds, *Tetrahedron Chem.* **2024**, 10,100064. DOI: 10.1016/j.tchem.2024.100064

[29] Domingo, L.R.: Ríos-Gutiérrez, M.; Revealing the Critical Role of Global Electron Density Transfer in the Reaction Rate of Polar Organic Reactions within Molecular Electron Density Theory. *Molecules* **2024**, 29, 1870. DOI: 10.3390/molecules29081870

[30] Bickelhaupt, F.M.; Fernández, I.; What defines electrophilicity in carbonyl compounds. *Chem. Sci.* **2024**, 15, 3980-3987. DOI: 10.1039/D3SC05595G

[31] Bickelhaupt, F.M.; Understanding reactivity with Kohn–Sham molecular orbital theory: E2–SN2 mechanistic spectrum and other concepts. *J. Comput. Chem.* **1999**, 20, 114–128. DOI:10.1002/(SICI)1096-987X(19990115)20:1%3C114::AID-JCC12%3E3.0.CO;2-L

[32] Bickelhaupt, F.M.; Baerends, E.J.; Kohn-Sham Density Functional Theory: Predicting and Understanding Chemistry., In Reviews in Computational Chemistry (eds K.B. Lipkowitz and D.B. Boyd). John Wiley & Sons, Inc. **2007**, pp 1-86.

[33] Mulliken, R.S.; Spectroscopy, molecular orbitals and chemical bonding. *Science* **1967**, 157, 13-24.

[34] Schrödinger, E.; An ondulatory theory of the mechanics of atoms and molecules. *Phys. Rev. B* **1926**, 28, 1049-1070. DOI: 10.1103/PhysRev.28.1049

[35] Hehre, W.J.; Radom, L.; Schleyer, P. v. R.; Pople, J. A.; *Ab initio molecular orbital theory*; Wiley, New York, **1986**.

[36] Jaramillo, P.; Domingo, L.R.; Chamorro, E.; Pérez. P.; A further exploration of a nucleophilicity index based on the gas-phase ionization potentials. *J. Mol. Struct. (Theochem)* **2008**, 865, 68-72. DOI: 10.1016/j.theochem.2008.06.022

[37] Chattaraj, P.K.; Roy, D.R.; Update 1 of: Electrophilicity Index, *Chem. Rev.* **2007**, 107, PR46–PR74. DOI: 10.1021/cr078014b

[38] Domingo, L.R.; Molecular Electron Density Theory: A Modern View of Reactivity in Organic Chemistry. *Molecules* **2016**, 21, 1319. DOI: 10.3390/molecules21101319

[39] Becke, A.D.; Edgecombe, K.E.; A simple measure of electron localization in atomic and molecular systems. *J. Chem. Phys.* **1990**, 92, 5397–5403. DOI: 10.1063/1.458517

[40] Bader, R.F.W.; Tang, Y.H.; Tal, Y.; Biegler-König, F.W.; Properties of atoms and bonds in hydrocarbon molecules. *J. Am. Chem. Soc.*, **1982**, 104, 946–952.

[41] Bader, R.F.W.; In *Atoms in Molecules: A Quantum Theory*, Oxford University Press, Oxford, New York, **1994**.

[42] Ríos-Gutiérrez, M.; Saz Sousa, A; Domingo, L.R. Electrophilicity and Nucleophilicity Scales at Different Computational Levels. *J. Phys. Org. Chem.* **2023**, e4503. DOI: 10.1002/poc.4503

[43] Silvi, B.; Savin, A.; Classification of chemical bonds based on topological analysis of electron localization functions. *Nature*, **1994**, 371, 683–686. DOI: 10.1038/371683a0

[44] Hammond, G. S.; A Correlation of Reaction Rates. *J. Am. Chem. Soc.* **1955**, 77, 334-338.

[45] Espinosa, E.; Alkorta, I.; Elguero, J.; Molins, E.; From weak to strong interactions: A comprehensive analysis of the topological and energetic properties of the electron density distribution involving X–H···F–Y system. *J. Chem. Phys.* **2002**, 117, 5529–5542. DOI: 10.1063/1.1501133

[46] J.-D. Chai and M. Head-Gordon, Long-range corrected hybrid density functionals with damped atom–atom dispersion corrections, *Phys. Chem. Chem. Phys.*, 2008, 10, 6615-6620. DOI: 10.1039/B810189B

[47] Schlegel, H. B.; Optimization of equilibrium geometries and transition structures. *J. Comput. Chem.*, **1982**, 3, 214-218. DOI: 10.1002/jcc.540030212

[48] Schlegel, H.B.; in *Modern Electronic Structure Theory*, ed. D. R Yarkony, World Scientific Publishing: Singapore, 1994.

[49] Fukui, K.; Formulation of the reaction coordinate. *J. Phys. Chem.*, **1970**, 74, 4161–4163.

[50] González, C.; Schlegel, H.B.; Reaction path following in mass-weighted internal coordinates. *J. Phys. Chem.*, **1990**, 94, 5523-5527.

[51] González, C.; Schlegel, H.B.; Improved algorithms for reaction path following: Higher-order implicit algorithms*. J. Chem. Phys.*, **1991**, 95, 5853-5860. DOI: 10.1063/1.461606

[52] Tomasi, J.; Persico, M.; Molecular interactions in solution: and overview of methods based on continuous distributions of the solvent. *Chem. Rev.*, 1994, **94**, 2027-2094.

[53] Simkin, B.Y.; Sheikhet, I.I.; Quantum chemical and statistical theory of solutions–computational approach, Ellis Horwood: London, **1995**.

[54] Cossi, M.; Barone, V.; Cammi, R.; Tomasi, J.; Ab initio study of solvated molecules: A new implementation of the polarizable continuum model. *Chem. Phys. Lett.*, **1996**, 255, 327-335. DOI: 10.1016/0009-2614(96)00349-1

[55] Cossi, M.; Barone, V.; Cammi, R.; Tomasi, J.; A new integral equation formalism for the polarizable continuum model: Theoretical background and applications to isotropic and anisotropic dielectrics. *J. Chem. Phys.*, **1997**, 107, 3032-3041. DOI: 10.1063/1.474659

[56] Barone, V.; Cossi, M.; Tomasi, J.; Geometry optimization of molecular structures in solution by the polarizable continuum model, *J. Comput. Chem.*, **1998**, 19, 404-417. DOI: 10.1002/(SICI)1096-987X(199803)19:4%3C404::AID-JCC3%3E3.0.CO;2-W

[57] Reed, A.E.; Weinstock, R.B.; Weinhold, F.; Natural population analysis. *J. Chem. Phys.*, **1985**, 83, 735-746. DOI: 10.1063/1.449486

[58] Reed, A.E.; Curtiss, L.A.; Weinhold, F.; Intermolecular interactions from a natural bond orbital, donor-acceptor viewpoint. *Chem. Rev.*, **1988**, 88, 899-926.

[59] Frisch, M.J.; Trucks, G.W.; Schlegel, H.B.; Scuseria, G.E.; Robb, M.A.; Cheeseman, J.R.; Scalmani, G.; Barone, V.; Petersson, G.A.; Nakatsuji, H.; et al. *Gaussian 16, Revision A.03*; Gaussian, Inc.: Wallingford, CT, USA, 2016.

[60] Noury, S.; Krokidis, X.; Fuster, F.; Silvi, B.; Computational tools for the electron localization function topological analysis. *Comput. Chem.*, **1999**, 23, 597-604. DOI: 10.1016/S0097-8485(99)00039-X

[61] Lu, T.; Chen, F. Multiwfn: A multifunctional wavefunction analyzer. *J. Comp. Chem.* **2012**, *33*, 580-592. DOI: 10.1002/jcc.22885

[62] Dennington, R.; Keith, T.A.; Millam, J.M.; GaussView, Version 6.1, Semichem Inc., Shawnee Mission, KS, *2016*.

[63] AIMAll (Version 19.10.12), Keith, T. A. TK Gristmill Software, Overland Park KS, USA, 2019 (aim.tkgristmill.com).